JOURNAL OF SOLID STATE CHEMISTRY **130,** 42–47 (1997)
ARTICLE NO. SC977270

Change in Crystal Structure and Electron Density by Introducing Oxygen in $YBa_2Cu_3O_y$ Single Crystal

Wen-Jye Jang, Hatsumi Mori, Masaya Watahiki, Setsuko Tajima, Naoki Koshizuka, and Shoji Tanaka

Superconductivity Research Laboratory, ISTEC 1-10-13 Shinonome Koto-ku, Tokyo 135, Japan

Received June 17, 1996; in revised form December 30, 1996; accepted January 7, 1997

The electron density map of tetragonal $YBa_2Cu_3O_6$ ($YBCO_6$) single crystal was investigated, in comparison with that of orthorhombic $YBa_2Cu_3O_{6.9}$ ($YBCO_{6.9}$). The crystal structure was determined by using four-circle X-ray diffraction data. The final values of the weighted reliability factor (R_W) and unweighted factor (R) were 0.027 and 0.024 for $YBCO_6$, which are small enough for analysis of the Fourier difference maps. The obtained Fourier difference map shows a wide negative electron density region around Cu1 and no clear peak in the vicinity of Cu2–O3 plane, except for a negative peak between Cu2 and O1. The introduction of O4 between two Cu1 atoms gives rise to substantial electron redistribution, creating negative and positive peaks around Cu1 and Cu2. There is no remarkable peak between Cu2 and O3 in $YBCO_6$, while a negative peak corresponding to the $3d_{x^2-y^2}$ orbital electrons is found in $YBCO_{6.9}$. The former result for $YBCO_6$ indicates that there is no clear bonding state within the CuO_2 plane.

INTRODUCTION

To understand the characteristic electronic state of the high-T_c superconducting oxides, an electron density map calculated from X-ray diffraction intensity data, particularly around the Cu–O conduction plane, would be of great use. Although a lot of structural analyses of $YBa_2Cu_3O_y$ ($YBCO_y$) have been reported for the tetragonal phase (1–6), the orthorhombic phase of twinned crystals (7–9), and the weakly twinned orthorhombic phase (10–11), there have been only a few reports on the electron density map (5, 8, 11, and 12). Recently we examined the electron density of $YBCO_{6.9}$ by using a high-quality twin-free crystal and clarified the difference in the density map between a and b directions (12). For deeper understanding of the meaning of the result for $YBCO_{6.9}$, it is important to compare it to that for nonsuperconducting $YBCO_6$ with the tetragonal structure. In this paper, we have carefully prepared an oxygen deficient $YBCO_6$ crystal and have measured its diffraction intensity, from which the Fourier (F) and Fourier difference (FD) maps were calculated. Comparing the maps with those of $YBCO_{6.9}$, we found that the additional oxygen O4 affects the whole electron density distribution and the bonding state. In $YBCO_{6.9}$, a clear bonding state consisting of positive and negative peaks in the FD map appears between O4 and Cu1, Cu1 and O1, O1 and Cu2, and Cu2 and O3.

EXPERIMENTAL

The $YBCO_y$ single crystal was grown by the top-seeded crystal pulling method. The as-grown crystal was cut into pieces with a size of $1.5 \times 1 \times 2$ mm and polished before annealing. The shaped crystal was annealed at 840°C in Ar atmosphere for 20 hr, resulting in the oxygen content of y close to 6. This annealing temperature was determined from the result of differential thermal analysis (DTA) that the YBCO compound decomposes at 864°C under Ar atmosphere. The composition ratio and the impurity contents were determined by an inductively coupled plasma atomic emission spectrometry (ICP).

Several pieces of single crystals with a size of $0.04 \times 0.04 \times 0.01$ mm were taken from the annealed crystal. They were covered by manicure liquid, just after being pulled out from a furnace, for protection against rapid oxygenation in air. The intensity data were collected by the 2θ-ω scan method, using a four-circle diffractometer (50 kV, 180 mA) with Mo$K\alpha$ radiation ($\lambda = 0.71069$ Å) monochromatized by graphite. The detailed X-ray experimental and refinement data are listed in Table 1, in comparison with our previous data for twin-free $YBCO_{6.9}$ (12). To compare these two, the occupancies of Y, Ba, Cu1, Cu2, O1, O2, and O3 were fixed at 1, 2, 1, 2, 2, 2, and 2 for both $YBCO_{6.9}$ and $YBCO_6$. The structure was calculated by using a Fourier analysis (13). Neutral atomic scattering factors were taken from Cromer and Waber (14). Anomalous dispersion effects were included in Fc (15); the values for $\Delta f'$ and $\Delta f''$ were from Creagh and McAuley (16). All calculations were carried out by using teXsan program (17).

0022-4596/97 $25.00

TABLE 1
Experimental and Refinement Data

Formula	$YBa_2Cu_3O_6$	$YBa_2Cu_3O_{6.9}$
Formula weight	650.22	664.62
Crystal size	Both are about $0.04 \times 0.04 \times 0.01$ mm^3	
Space group	*P4/mmm*	*Pmmm*
Z value	1	1
μ(Mo$K\alpha$)	279.65 cm^{-1}	282.77 cm^{-1}
Radiation	0.71069 Å (Mo$K\alpha$) graphite monochromated	
Diffractometer	Rigaku AFC5R	
Temperature	Room temperature	
Scan type	ω-2θ	
Scan rate	4.0°/min	
Scan width	$1.68° + 0.3$	$1.78° + 0.3$
2θ range	$4° \le 2\theta \le 120°$	
Sphere of data	$\pm h, \pm k, \pm l$	$h, k, \pm l$
No. reflections	5852	3072
Independent	884	1574
Corrections	Loretnz–polarization and absorption (φ-scan)	
Secondary extinction	4.97×10^{-6}	3.36×10^{-6}
Structure solution	Direct methods	
Refinement	Full-matrix least-squares	
No. observations	614 ($I > 5.0\sigma(I)$)	1147 ($I > 5.0\sigma(I)$)
No. variables	19	32
Residuals R; R_w	0.027; 0.024	0.027; 0.032
Max. shift/error in final cycle	0.003	0.002

RESULTS AND DISCUSSIONS

The crystal annealed at 840°C in Ar gas shows a very weak superconducting transition around 50 K in the susceptibility measurement. This means that the oxygen content y is not completely reduced to 6 in some parts of this crystal, presumably in the center. But a small shaped crystal piece which was cut from outside of this crystal shows no oxygen atom at the Cu–O chain site (the O4 site) in the refinement result of the X-ray analysis.

The composition ratio determined by the ICP measurement was $Y_1Ba_{2.06}Cu_{0.37}O_y$ with a small amount of impurity such as 0.04 wt% of Mg and 0.02 wt% of Sr. The structure refinement for the site multiplicity in the X-ray analysis of the fully oxygenated crystal showed that the chemical formula can be written as $Y_1Ba_{2.02}Cu_{2.98}O_{6.92}$ by fixing the occupancies of Y, O1, O2, and O3 (12). Since the composition ratio (Y : Ba : Cu) determined by both the ICP and X-ray measurements is very close to 1 : 2 : 3 within an experimental error, it is justified to regard our YBCO single crystal as stoichiometric. Thus, we fixed the occupancies of Y, Ba, Cu1, Cu2, O1, and O3 at 1, 2, 1, 2, 2, 2, and 4 for $YBCO_6$ in this study, because all these crystal pieces were cut out from the same as-grown crystal. In comparison, we refined the data again for the $YBCO_{6.9}$ phase (Table 2), fixing the occupancies of all elements, except for O4, to be the same as for $YBCO_6$, and found that all the parameters are not much different from our previous results for $Y_1Ba_{2.02}Cu_{2.98}O_{6.92}$ in which only the occupancies of Y, O1, O2, and O3 were fixed (12).

The obtained crystal data for $YBCO_6$ are as follows: $Mr = 650.2$; tetragonal; *P4/mmm* (No. 123); $a = 3.8600(7)$, $c = 11.844(1)$ Å, $V = 176.46(5)$ Å; $Z = 1$, $D_x = 6.118$ Mg^{-3}; λ(Mo$K\alpha$) = 0.71069 Å; μ(Mo$K\alpha$) = 279.65 cm^{-1}. All of the thermal parameters have converged on reasonable values, which are larger than those for the $YBCO_{6.9}$ crystal (Table 2), indicating that the $YBCO_6$ phase is much more unstable than the $YBCO_{6.9}$ phase. The unit cell volume of the $YBCO_6$ phase is larger than that of $YBCO_{6.9}$ even though there is additional oxygen at the O4 site in $YBCO_{6.9}$ (Fig. 1). This demonstrates that the O4 atom plays the role of stabilizer in the $YBCO_y$ crystal. $YBCO_6$ bulk crystal was easily decomposed into the green phase (Y_2BaCuO_5) and some other phases in air a few weeks after annealing, whereas $YBCO_{6.9}$ crystal was not decomposed even after annealing at 500°C in oxygen gas. Another possible reason for the larger thermal parameters of $YBCO_6$ is a slight mixture of orthorhombicity due to the remaining oxygen at the O4 site, which cannot be prevented because it is very hard to get a perfectly reduced crystal $YBCO_6$.

Interatomic distances and angles for two YBCO crystals are compared in Table 3. It should be emphasized that the distance of Cu1–O1 for $YBCO_6$ (1.803 Å) is shorter than that of $YBCO_{6.9}$ (1.848 Å) which is shorter than the other Cu–O bond distances. On the other hand, the Cu2–O1 distance for $YBCO_6$ (2.473 Å) is longer than that of $YBCO_{6.9}$ (2.313 Å). This means that the apical oxygen O1 shifts from the Cu1 side to the Cu2 side with the introduction of O4. Other effects of O4 on the bond distances are the elongation of Ba–O3 and the shortening of Y–O3, while the Y–O2 distance does not change. The Cu2–O3–Cu2 angle of 167.3° in $YBCO_6$ decreases down to 164.3° for O3 and 163.4° for O2 in $YBCO_{6.9}$. This is due to the shift of the Cu2 cation toward the O1 anion (Fig. 1). These shifts of Cu2 and O1 were also reported by M. Marezio (18), based upon the X-ray powder diffraction (PWD) method.

Although residual peaks with $\Delta\rho = 1.4$ eA^{-3} are observed between two Cu1 in the Fourier difference map (Fig. 2a), these electron peaks do not originate from O4 since the refinement of the structure analysis including O4 has failed.

The final cycle of full-matrix least-squares refinement was converged at the maximum shift/error of less than 0.003. The unweighted and weighted R values are represented as

$$R = \sum ||F_o| - |F_c|| / \sum |F_o|$$

and

$$R_w = \sqrt{\sum \omega(|F_o| - |F_c|)^2 / \sum \omega F_o^2},$$

where F_o is the experimentally observed crystal structure factor and F_c is the calculated crystal structure factor for the

TABLE 2
Atomic Coordinates, Anisotropic and Equivalent Isotropic Temperature Coefficients, and Site Occupation Factors

Formula: $Y_1Ba_2Cu_3O_6$ $a = 3.8600(7)$, $c = 11.844(1)$ Å, $V = 176.46(5)$ Å^3 (for tetragonal crystal)

Atom	Y	Ba	Cu1	Cu2	O1	O3
x	0.5	0.5	0	0	0	0
y	0.5	0.5	0	0	0	0.5
z	0.5	0.19522(3)	0	0.36103(6)	0.1522(3)	0.3792(2)
U_{11}[a]	0.0057(1)	0.00824(6)	0.0122(2)	0.0046(1)	0.0140(9)	0.0081(9)
U_{22}	$= U_{11}$	$= U_{11}$	$= U_{11}$	$= U_{11}$	$= U_{11}$	0.0044(8)
U_{33}	0.0077(2)	0.00890(9)	0.0095(3)	0.0111(2)	0.012(1)	0.0119(9)
B_{eq}[b]	0.502(5)	0.668(2)	0.890(7)	0.534(4)	1.05(3)	0.64(3)
occ.	1	2	1	2	2	4

Formula: $Y_1Ba_2Cu_3O_{6.91(1)}$ $a = 3.8278(7)$, $b = 3.8952(7)$, $c = 11.711(2)$ Å, $V = 174.61(5)$ Å^3 (for twin-free orthorhombic crystal)

Atom	Y	Ba	Cu1	Cu2	O1	O2	O3	O4
x	0.5	0.5	0	0	0	0.5	0	0
y	0.5	0.5	0	0	0	0	0.5	0.5
z	0.5	0.18469(2)	0	0.35525(4)	0.1578(2)	0.3791(2)	0.3781(2)	0
U_{11}	0.0046(1)	0.00641(6)	0.0074(2)	0.0033(1)	0.0103(8)	0.0036(7)	0.0061(7)	0.029(3)
U_{22}	0.0043(1)	0.00507(5)	0.0060(2)	0.0034(1)	0.0106(8)	0.0069(7)	0.0038(6)	0.006(1)
U_{33}	0.0043(1)	0.00637(5)	0.0034(2)	0.0070(7)	0.0063(7)	0.0089(8)	0.0080(7)	0.012(2)
B_{eq}	0.348(5)	0.470(2)	0.443(7)	0.359(5)	0.72(3)	0.51(3)	0.47(3)	1.23(8)
occ.	1	2	1	2	2	2	2	0.91(1)

[a] $T_a = \exp\{-2\pi^2(a^{*2}U_{11}h^2 + b^{*2}U_{22}k^2 + c^{*2}U_{33}l^2)\}$, T_a: general temperature factor.
[b] $B_{eq} = \frac{8}{3}\pi^2\{U_{11}(aa^*)^2 + U_{22}(bb^*)^2 + U_{33}(cc^*)^2\}$.

model structure. The obtained R values are listed in Table 1. The FD maps were drawn using the $|F_o| - |F_c|$ values obtained in the final steps of the refinement. Figures 2 and 3 show the FD maps and the F maps, respectively. The contour interval for mapping is 0.69 eÅ^{-3} for the FD maps and 1 eÅ^{-3} for the F maps. In the FD maps, a region with positive and/or negative $\Delta\rho = |F_o| - |F_c|$ is represented by a solid and/or a dashed curve, respectively. The reliability of

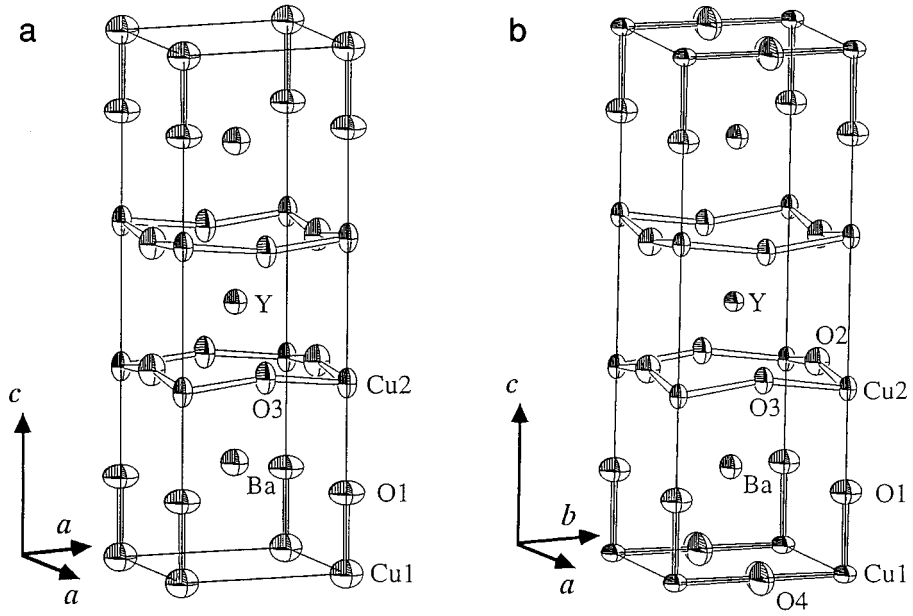

FIG. 1. (a) Tetragonal $YBCO_6$ and (b) orthorhombic $YBCO_{6.9}$ crystal structures at 90% probability level for data in Table 2.

TABLE 3
Interatomic Distances (Å) and Angles of Tetragonal $YBa_2Cu_3O_6$ Compared with Twin-Free Orthorhombic $YBa_2Cu_3O_{6.9}$ Crystals

Tetragonal crystals: $a = 3.8600(7)$, $c = 11.844(1)$ Å, $V = 176.46(5)$ Å^3

Ba–O1	2.7766(9) × 4	[O1	2.7487(4) × 4][a]	Cu1–O1	1.803(4) × 4	[O1	1.848(3) × 4]
–O3	2.911(2) × 4	[O2	2.996(2) × 2]			[O1	1.9476(3) × 1.8]
		[O3	2.966(2) × 2]				
		[O4	2.8881(2) × 1.8]				
				Cu2–O1	2.473(4) × 1	[O1	2.313(3) × 1]
Y–O3	2.403(1) × 8	[O2	2.408(2) × 4]	–O3	1.9419(4) × 4	[O2	1.9342(4) × 2]
		[O3	2.387(2) × 4]			[O3	1.9660(5) × 2]
Cu2–O3–Cu2	167.3(1)°	[Cu2–O2–Cu2	163.4(2)°]				
		[Cu2–O3–Cu2	164.3(2)°]				

[a] The square bracket data is for a twin-free orthorhombic crystal: $a = 3.8278(7)$, $b = 3.8952(7)$, $c = 11.711(2)$ Å, $V = 174.61(5)$ Å^3.

the electron density map was checked by examining the crystal structure for the atomic scattering factor of Y^{3+}, Ba^{2+}, Cu^{2+}, and O^{2-}, as well as that for neutral atoms. Since both analyses afforded the same F and FD maps, it is considered that our calculated electron density based on the crystal structure analysis is not sensitive to the above parameters and thus is reliable.

If we assume that the formal valences of oxygen, Y, and Ba are -2, $+3$, and $+2$, respectively, in $YBCO_6$, the valences of Cu2 and Cu1 are expected to be $+2$ and $+1$. When oxygen is inserted at the O4 site, the Cu1 valence is expected to become larger. Actually in $YBCO_{6.9}$, the Cu1 valence is observed to be larger than $+2$ (18). A FD map shows a deviation of electron density from the model in which all the atoms are neutral and located at the positions shown in Table 2. Therefore, a positive (negative) peak indicates a higher (lower) electron density region than the neutral valence model. A remarkable difference between $YBCO_6$ and $YBCO_{6.9}$ in the FD maps is that there is no clear peak in $YBCO_6$ except for a negative peak around Cu2, while many peaks are observed in $YBCO_{6.9}$. This demonstrates that addition of the O4 atom dramatically changes the electron distribution and creates its substantial overlap between the atoms. The effect of the introduction of O4 is interpreted as follows. Since the incorporated anion O4 wrests electrons from Cu1, the FD electron density around the Cu1 cation becomes more negative along the *b*-axis (Fig. 2c). This gives rise to the shift of the positive electron peak between Cu1 and O1 toward the Cu1 cation along the *c*-axis. Marezio (18) concluded that the average

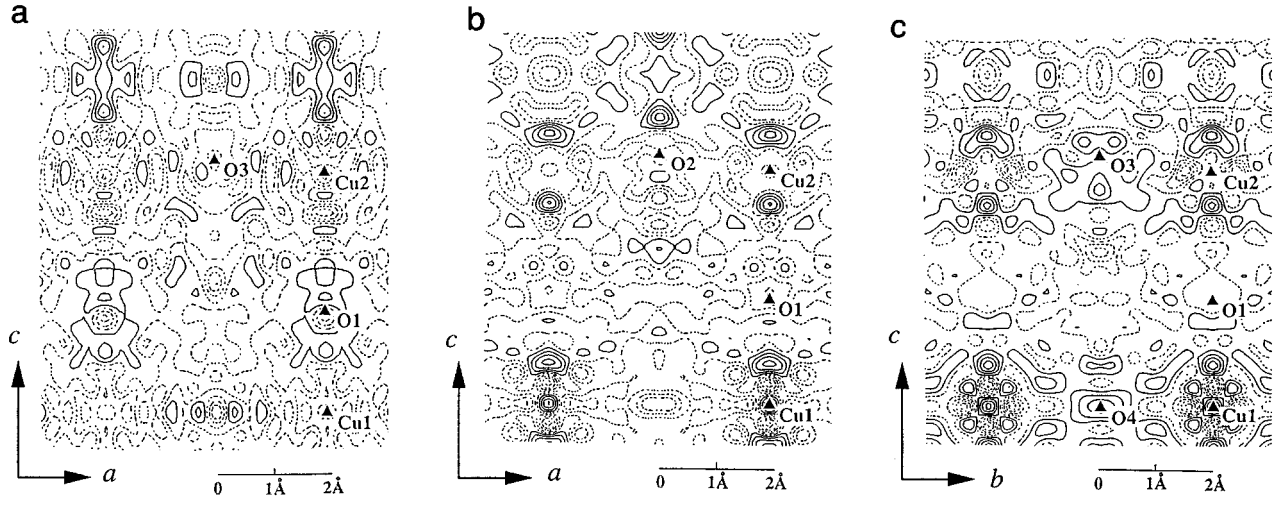

FIG. 2. Fourier difference maps (a) for the tetragonal $YBCO_6$ crystal in the (100) plane at $x = 0$, (b) for the orthorhombic $YBCO_{6.9}$ crystal in the (010) plane at $y = 0$, and (c) in the (100) plane at $x = 0$. Contour interval is 0.69 eÅ^{-3}. Contours in positive $\Delta\rho$ regions are represented by solid curves and those in negative $\Delta\rho$ regions by dashed curves. Curve for $\Delta\rho = 0$ is omitted.

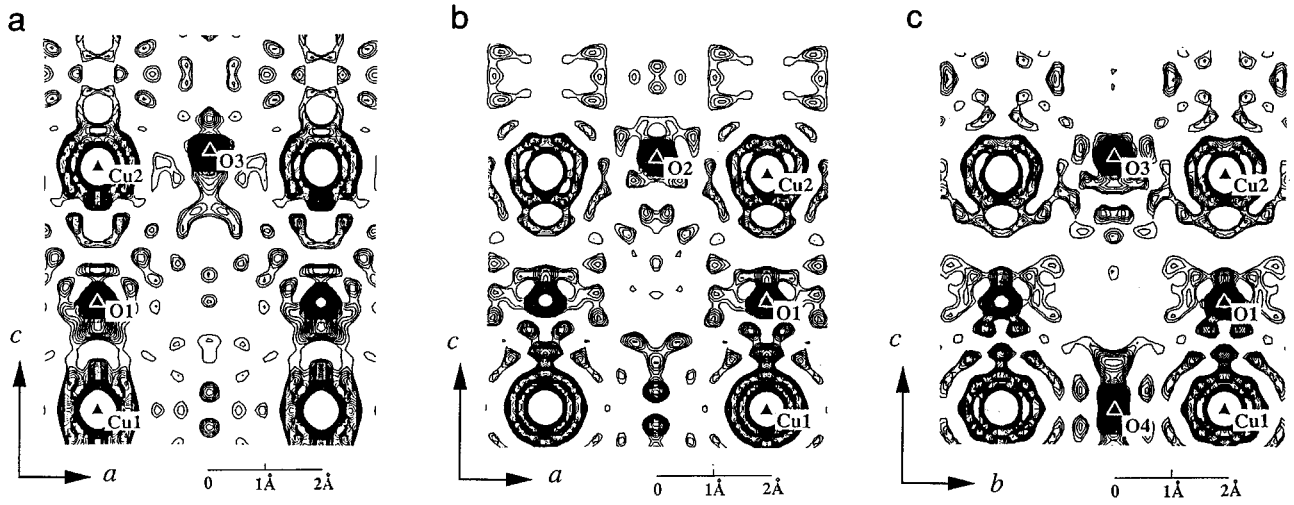

FIG. 3. Fourier maps for the data in Fig. 2, i.e., (a) for the tetragonal $YBCO_6$ crystal in the (100) plane at $x = 0$, (b) for the orthorhombic $YBCO_{6.9}$ crystal in the (010) plane at $y = 0$, and (c) in the (100) plane at $x = 0$. Contour interval is 1 $e\text{Å}^{-3}$.

valence of the Cu1 cation increases from $+1.3$ to $+2.4$, estimated from the bond distance. The positive peak with $\Delta\rho = 2.8\ e\text{Å}^{-3}$ is 0.7 Å away from Cu1 in the c direction. Between O1 and Cu2, the positive peak with $\Delta\rho = 2.8\ e\text{Å}^{-3}$ also becomes strong and shifts toward Cu2, which results from the shift of O1 toward Cu2.

Figures 2b and 2c show that there is a residual electron density in the $3d_{yz}$ orbital of Cu1, but not in d_{xy}, d_{zx}, and $d_{x^2-y^2}$ orbitals. This indicates anisotropic electron distribution, which is caused by the O4–Cu1 bonding. In the Cu2–O3–Cu2 layer, there is no obvious peak in the $YBCO_6$ phase. In $YBCO_{6.9}$, the electrons around Cu2 do not form an original dumbbell shape, but are localized as a lone pair being separated from the negative region between Cu2 and O2. The negative peak with $\Delta\rho = -2.8\ e\text{Å}^{-3}$, being 0.58 Å away from Cu2, indicates that the Cu2 $d_{x^2-y^2}$ orbital is unfilled. A similar negative peak between Cu2 and O3 is also observed in $Tl_2Ba_2CaCu_2O_8$ superconductor (19). Compared with the bonding between Cu1–O1, the bonding electrons for Cu2–O2/O3 are not clearly observed in both $YBCO_6$ and $YBCO_{6.9}$. In $YBCO_{6.9}$, although a wide positive region around O3 seems to suggest a bonding like Cu1–O4, it does not form a peak just between O3 and Cu2. From these observations it is concluded that the electron peaks created by introducing O4 are not located just within the Cu2–O2/O3 layer but slightly shifted in the c direction, which suggests a characteristic bonding between Cu2 and O2/O3.

We can also see a remarkable difference between $YBCO_6$ and $YBCO_{6.9}$ in the F maps shown in Fig. 3. The distribution of $3d$ electrons in the outer shell of the Cu1 atom becomes more circular when oxygen is introduced at the O4 site. For $YBCO_{6.9}$ the distribution of $3d_{yz}$ orbital electrons in the bc plane is more protuberant than the d_{zx} orbital electrons in the ac plane. It is also observed in Fig. 3c that the electron distribution around O4 is overlapped with that of O1. This is known as dsp^2 hybrids; the four bonds lie in the same plane and are directed toward the corners of a square. The overlap of electron distribution becomes pronounced not only between Cu1 and O4 but also between Cu2 and O2/O3 in $YBCO_{6.9}$, whereas the $3d$ orbital around Cu2 is not overlapped with the O3 orbital in $YBCO_6$. This results in the homogeneous FD map for $YBCO_6$ without any sharp peak.

CONCLUSION

A crystal structure and an electron density map of tetragonal $YBCO_6$ were obtained by using the four-circle X-ray diffraction method. They were compared with the results for a twin-free orthorhombic $YBCO_{6.9}$ single crystal with new refinement. All thermal parameters of $YBCO_6$ are larger than those of $YBCO_{6.9}$, indicating that the former phase is much more unstable than the latter phase. The final values of the weighted reliability factor (R_w) and unweighted factor (R) were 0.027 and 0.024 for $YBCO_6$ and 0.032 and 0.027 for $YBCO_{6.9}$, which are small enough for analysis of FD maps. The F maps and the FD maps have revealed differences of the electron distribution and the bonding nature of these two phases. In the FD maps for $YBCO_6$, no clear peak is observed except for a negative peak around Cu2, while pronounced electron density peaks are observed between the atoms in $YBCO_{6.9}$. This is not caused by an increase in electron number but by the electron redistribution due to the introduction of O4. The main differences in the electron

distribution between the two phases are as follows:

(1) The negative electron density region spreads out around Cu1 without positive peak in the FD map for $YBCO_6$, while O4 takes the electrons from Cu1 in $YBCO_{6.9}$, creating the negative peaks around Cu1, and the strong positive peak between O1 and Cu1 shifts toward Cu1.

(2) A negative peak with $\Delta\rho = -2.8\ e\text{Å}^{-3}$ is observed about 0.7 Å away from Cu2 toward O1 in $YBCO_6$, indicating a weak bonding between Cu2 and O1. When O4 is introduced, O1 shifts toward Cu2. As a result the positive peak between O1 and Cu2 becomes strong and shifts toward Cu2.

(3) The bonding electrons between Cu2–O2 and Cu2–O3 are not clearly seen in both phases. The positive peaks in $YBCO_{6.9}$ are not located just within the Cu2–O2/O3 plane but deviated in the *c* direction, suggesting its characteristic bonding state.

(4) The electron distribution around Cu2 is not overlapped with that for O3 in $YBCO_6$. This results in the homogeneous FD maps in the Cu2–O3 layer without any peak. In contrast, there is a negative peak between Cu2 and O3 in the FD map of $YBCO_{6.9}$, corresponding to the unified $3d_{x^2-y^2}$ orbital.

ACKNOWLEDGMENT

This work was supported by the New Energy and Industrial Technology Development Organization for the R&D of Industrial Science and Technology Frontier Program.

REFERENCES

1. G. Roth, B. Renker, G. Heger, M. Hervieu, B. Domenges, and B. Raveau, *Z. Phys. B* **69,** 53 (1987).
2. I. Nakai, S. Sueno, F.P. Okamura, and A. Ono, *Jpn. J. Appl. Phys.* **26,** L788 (1987).
3. R. M. Hazen, L. W. Finger, R. J. Angel, C. T. Prewitt, N. L. Ross, H. K. Mao, C. G. Hadidacos, P. H. Hor, R. L. Meng, and C. W. Chu, *Phys. Rev. B* **35,** 7238 (1987).
4. M. F. Garbauskas, R. W. Green, R. H. Arendt, and J. S. Kasper, *Inorg. Chem.* **22,** 871 (1988).
5. S. Sasaki, Z. Inoue, N. Iyi, and S. Takekawa, *Acta Crystallogr. B* **48,** 393 (1992).
6. S. Sato, I. Nakada, T. Kohara, and Y. Oda, *Acta Crystallogr. C* **44,** 11 (1988).
7. S. Sato, I. Nakada, T. Kohara, and Y. Oda, *Jpn. J. Appl. Phys.* **26,** L663 (1987).
8. R. H. Buttner, E. N. Maslen, and N. Spadaccini, *Acta Crystallogr. B* **48,** 21 (1992).
9. A. Simon, K. Trubenbach, and H. Borrmann, *J. Solid State Chem.* **106,** 128 (1993).
10. K. Brodt, H. Fuess, E. F. Paulus, W. Assmus, and J. Kowalewski, *Acta Crystallogr. C* **46,** 354 (1990).
11. J. D. Sullivan, P. Bordet, M. Marezio, K. Takenaka, and S. Uchida, *Phys. Rev. B* **48,** 10638 (1993).
12. W.-J. Jang, H. Mori, M. Watahiki, S. Tajima, N. Koshizuka, and S. Tanaka, *J. Solid State Chem.* **122,** 371 (1996).
13. P. T. Beurskens, G. Adamiraal, G. Beurskens, W. P. Bosman, S. Garcia-Granda, R. O. Gould, J. M. M. Smiths, and C. Smykalla, "The DIRDIF program system," technical report of the Crystallography Laboratory, University of Nijmegen, The Netherlands.
14. D. T. Cromer and J. T. Waber, "International Tables for X-ray Crystallography," Vol. IV, Table 2.2 A. The Kynoch Press, Birmingham, England, 1974.
15. J. A. Ibers and W. C. Hamilton, *Acta Crystallogr.* **17,** 781 (1964).
16. D. C. Creagh and W. J. McAuley, *in* "International Tables for Crystallography" (A. J. C. Wilson, Ed.), Table 4.2.6.8, p. 219, Kluwer, Boston, 1992.
17. "Crystal Structure Analysis Package," Molecular Structure Corporation, 1985, 1992.
18. M. Marezio, *Acta Crystallogr. A* **47,** 640 (1991).
19. S. Sasaki, T. Mori, K. Kawaguchi, and M. Nakao, *Physica C* **247,** 289 (1995).